Multiple-Mode Structural Vibration Control Using Negative Capacitive Shunt Damping

Chul Hue Park*, Hyun Chul Park

Department of Mechanical Engineering, Pohang University of Science and Technology, San 31 Hyoja Dong, Pohang, KyungBuk, 790-784, Korea

This paper deals with a novel shunt circuit, which is capable of suppressing multimode vibration amplitudes by using a pair of piezoceramic patches. In order to describe the characteristic behaviors of a piezoelectric damper connected with a series and a parallel resistor-negative capacitor branch circuit, the stiffness ratio and loss factor with respect to the non-dimensional frequency are considered. The mechanism of the shunt damper is also described by considering a shunt voltage constrained by shunt impedance. To obtain a guideline model of the piezo/beam system with a negative capacitive shunting, the governing equations of motion are derived through the Hamilton's principle and a piezo sensor equation as well as a shunt-damping matrix is developed. The theoretical analysis shows that the piezo/beam system combined with a series and a parallel resistor-negative capacitor branch circuit developed in this study can significantly reduce the multiple-mode vibration amplitudes over the whole structural frequency range.

Key Words : Vibration Control, Shunt Circuit, Negative Capacitance, Piezoelectric Material

1. Introduction

Multiple-mode structural vibration control using a shunt circuit has received enormous attention due to its desirable vibration reduction characteristics and low power requirement. Browning and Wynn (1993) performed an experiment that achieves simultaneous reduction of multiple vibration modes by applying multiple piezoceramic elements bonded to the surface of a plate with a resonant shunting technique. Hollkamp (1994) developed a theory to suppress multiple modes by using a single piezoelectric element coupled with a multimode shunt network. Wu (1998) presented a shunt network for damping multiple vibration modes by employing blocking circuits that act as a filter for screening unwanted current frequencies. Moon et al.(2002) investigated the nonlinear flutter problem of a composite panel by employing in turn one shunt circuit and two independent inductor-resistor shunt circuits.

A new multiple-mode vibration damper is introduced in this paper by using negative capacitive shunting ; one is connected to the terminals of a PZT with a resistor-negative capacitor shunt branch circuit in series, the other is connected with it in parallel as shown in Fig. 1. The negative capacitance circuit provides the negative capacitance of a magnitude that cancels the internal capacitance of the PZT patch to maximize the energy dissipation (Forward, 1979). Therefore, the electrical impedance of a shunted piezo/beam system reduces to that of resistance, which is frequency independent and makes it possible to control multiple vibration modes.

A piezo patch attached on the beam with a series resistor-negative capacitive shunting is designed to control the vibration amplitudes in the low frequency range. The other patch bonded below the beam with parallel resistor-negative

* Corresponding Author,
E-mail : drparkch@postech.ac.kr
TEL : +82-54-279-2962; **FAX** : +82-54-279-5899
Department of Mechanical Engineering, Pohang University of Science and Technology, San 31 Hyoja Dong, Pohang, KyungBuk, 790-784, Korea. (Manuscript **Received** December 9, 2002; **Revised** July 30, 2003)

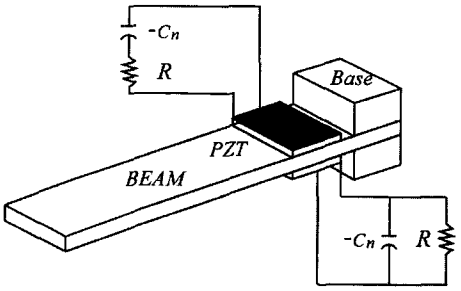

Fig. 1 A schematic drawing of the shunted piezo/beam system

capacitive shunting is for suppressing vibration modes in the high frequency range. The equations of motion of the shunted piezo/beam system are formulated using Hamilton's principle. Assumed shape functions, satisfying the boundary conditions, are used to analyze the flexural motion of the cantilevered piezo/beam system. The obtained result shows that negative capacitive shunting provides an effective means for multimode vibration damping over a broadband structural frequency range.

2. Characteristics of a Negative Capacitive Shunting

The characteristic behaviors of a negative capacitive shunting can be expressed in terms of the non-dimensional mechanical impedance, $\bar{Z}_{ME}$. It is expressed in terms of the stiffness ratio, $\bar{E}(\omega)$, and material loss factor, $\eta(\omega)$, which are frequency dependent.

$$\bar{Z}_{ME}=\bar{E}(\omega)[1+\eta(\omega)] \tag{1}$$

In order to develop the non-dimensional mechanical impedance of piezo shunt, the current and the strain are defined as follows:

$$I=\frac{1}{Z_{PZT}}V_{SH}+sAdT \tag{2}$$

$$S=\frac{d}{t}V_{SH}+s^{E}T \tag{3}$$

where T_{PZT} is the impedance of piezoelectric material given by

$$Z_{PZT}=\frac{1}{sC_p^T} \tag{4}$$

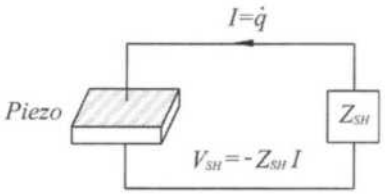

Fig. 2 Feedback shunt voltage generated due to shunt impedance

where C_p^T is the internal capacitance of PZT measured at constant stress and s is the Laplace parameter. The current, I, is generated by external stress and is fed back into the PZT and V_{SH} is the voltage across the shunt impedance as shown in Fig. 2. In Eq. (2), A, d, and t denote the diagonal matrix of the surface area of a piezo material, piezo material constant, and thickness matrix of the piezo bar, respectively. In Eq. (3), S and T denote the mechanical strain and stress matrices. According to Fig. 2, the shunt voltage is given by

$$V_{SH}=-Z_{SH}I \tag{5}$$

where Z_{SH} is the electrical impedance of the shunt circuit. The shunt voltage can be rewritten by substituting the current in Eq. (5) into Eq. (2).

$$V_{SH}=-sAZ_{EL}dT$$

where

$$\frac{1}{Z_{EL}}=\frac{1}{Z_{PZT}}+\frac{1}{Z_{SH}} \tag{6}$$

Substituting Eq. (6) into mechanical strain equation [Eq. (3)], the shunt strain can be obtained by

$$\begin{aligned}S_{SH}&=\frac{d}{t}(-sAZ_{EL}dT)+s^{E}T\\&=s^{E}T(1-sC_p^Tk_{ij}^2Z_{EL})=s^{E}T(1-k_{ij}^2\bar{Z}_{EL})\end{aligned} \tag{7}$$

where $k_{ij}^2=\frac{d_{ij}^2}{s^E\epsilon_i^T}$ and the non-dimensional electrical impedance is defined as $\bar{Z}_{EL}=Z_{EL}/Z_{PZT}$. Following the definition of the non-dimensional mechanical impedance, $\bar{Z}_{ME}$, it is expressed as (Hagood and von Flotow, 1991)

$$\bar{Z}_{ME}=\frac{S^D}{S_{SH}}=\frac{(1-k_{ij}^2)}{(1-k_{ij}^2\bar{Z}_{EL})} \tag{8}$$

where S^D is the piezoelectric material compliance

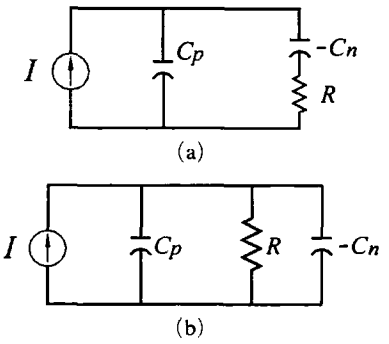

Fig. 3 Circuit models of piezoceramic with (a) a series and (b) a parallel negative capacitive shunt branch circuit

taken at constant electrical displacement and S_{SH} is the shunted piezoelectric compliance. The non-dimensional electrical impedance, $\bar{Z}_{EL}$, for the negative capacitive shunting can be obtained by considering the PZT circuit model with a resistor-negative capacitor branch circuit as shown in Fig. 3.

In the series case,

$$\bar{Z}_{EL}^{SE}=\frac{(sRC_n^T-1)\,C_p^T}{C_n^T-C_p^T+sRC_p^TC_n^T} \tag{9a}$$

In the parallel case,

$$\bar{Z}_{EL}^{PA}=\frac{sC_n^TR}{1+sC_n^TR-sRC_n^TR} \tag{9b}$$

where $-C_n^T$ is an external negative capacitor value, which should be the same as that of the inherent piezoelectric transducer capacitance C_p^T, for impedance matching. Substituting Eq. (9) into Eq. (8) and equating C_p^T to C_n^T, the non-dimensional mechanical equation, $\bar{Z}_{ME}$, reduces to:

In the series case,

$$\bar{Z}_{ME}^{SE}=\frac{\rho_i^2}{k_{ij}^4+\rho_i^2}+i\,\frac{\rho k_{ij}^2}{k_{ij}^4+\rho_i^2} \tag{10a}$$

In the parallel case,

$$\bar{Z}_{ME}^{PA}=\frac{(1-k_{ij}^2)^3}{(1-k_{ij}^2)^2+(k_{ij}^2\rho_i)^2}+i\,\frac{\rho k_{ij}^2(1-k_{ij}^2)^2}{(1-k_{ij}^2)^2+(k_{ij}^2\rho_i)^2} \tag{10b}$$

where ρ_i is the non-dimensional frequency and is defined by

$$\rho_i=R_iC_p^S\omega=\omega/\omega_e \tag{11}$$

and C_p^S is defined as $C_p^S=C_p^T(1-k_{ij}^2)$. From Eq. (10), the non-dimensional mechanical impedance, $\bar{Z}_{ME}$, is a complex number and dependent on the non-dimensional frequency. According to Eq (1), the stiffness ratio (the ratio of shunted stiffness to open circuit stiffness) $\bar{E}$ and the material loss factor η can be derived as follows:

In the series case,

$$\bar{E}^{SE}(\omega)=\mathrm{Re}(\bar{Z}_{ME}^{SE})=\frac{\rho_i^2}{k_{ij}^4+\rho_i^2},\qquad \eta^{SE}=\frac{\mathrm{Im}(\bar{Z}_{ME}^{SE})}{\mathrm{Re}(\bar{Z}_{ME}^{SE})}=\frac{k_{ij}^2}{\rho_i} \tag{12a}$$

In the parallel case,

$$\bar{E}^{PA}(\omega)=\mathrm{Re}(\bar{Z}_{ME}^{PA})=\frac{(1-k_{ij}^2)^3}{(1-k_{ij}^2)^2+(k_{ij}^2\rho_i)^2},\qquad \eta^{PA}=\frac{\mathrm{Im}(\bar{Z}_{ME}^{PA})}{\mathrm{Re}(\bar{Z}_{ME}^{PA})}=\frac{\rho k_{ij}^2}{(1-k_{ij}^2)^2} \tag{12b}$$

The stiffness ratio and loss factor of a negative capacitive shunting are plotted versus the non-dimensional frequency in Fig. 4 for both branch circuits. The electromechanical coupling coefficient k_{31}, used for the present analysis is 0.33. It is clear that the stiffness ratio decreases with increasing non-dimensional frequency and goes to zero in the parallel case. On the contrary, the stiffness ratio starts from zero and increases with increasing non-dimensional frequency in the series case.

The electromechanical coupling coefficient k_{ij} is commonly used as a criterion for measuring the damping capability of a piezoelectric material and is defined as the ratio of the stored mechanical (electrical energy) to the total energy imposed and described in the following form (Lesieutre and Davis, 1997):

$$k_{ij}^2=\frac{e^2}{c^E\varepsilon_i^S+e^2} \tag{13}$$

where c^E is a matrix of elastic coefficients at constant electric field, e is a matrix of piezoelectric coefficient, and ε_i^S is a matrix of dielectric permittivity at constant strain. From Eq. (13), as the elastic coefficient approaches zero, the electromechanical coupling coefficient becomes unity.

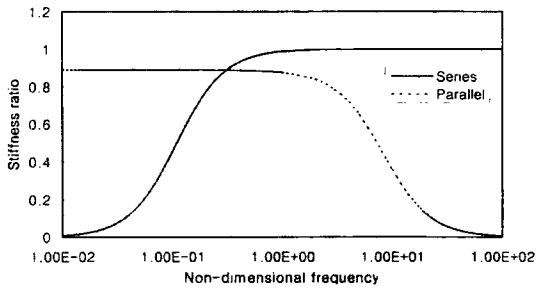

(a) Stiffness ratio

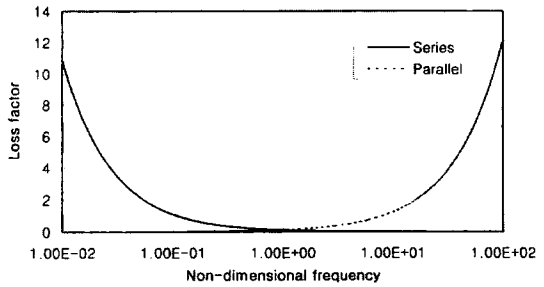

(b) Loss factor

Fig. 4 Material properties of a series and a parallel negative capacitive shunt

This means that the energy conversion factor between the mechanical energy and electrical energy is 100%. According to Fig. 4(a), this phenomenon occurs at high frequencies in the parallel case and at low frequencies in the series case.

Figure 4(b) certifies that the material loss factor increases with increasing the non-dimensional frequency in the parallel shunt branch circuit and decreases with increasing the non-dimensional frequency in the series shunt branch circuit. This fact shows that the parallel shunt branch circuit can obtain more damping in high frequency range and the series shunt branch circuit can do so in low frequency range.

3. General Modeling of Shunted Actuator

The piezo shunt circuit generates an additional damping matrix that can be added to the equations of motion of a structural system. A pair of piezoelectric actuator/sensor equations (Hagood et al, 1990) is used to derive an additional shunt-damping matrix.

Actuator equation :

$$M\ddot{w}+C\dot{w}+Kw=f_{ext}+\theta V_{SH} \tag{14}$$

Sensor equation :

$$q=\theta^T w+C_p V_{SH} \tag{15}$$

where M, C, and K are the mass, damping, and stiffness matrices of the piezo/beam system measured at constant field (short circuit). Hence, the system stiffness consists of a base structure stiffness and a short circuited piezoelectric stiffness, that is, $K=K_S+K_p^E$. In the sensor equation, q is the piezoelectric charge matrix and θ is the electromechanical coupling matrix. This piezoelectric actuator/sensor equation accounts for the effects of dynamic coupling between a structure and an electrical network through the piezoelectric effect. A current equation can be obtained by differentiating the sensor equation [Eq. (15)]. Substituting it into the shunt voltage equation as shown in Fig. 2, we can redefine it as follows :

$$\begin{aligned} V_{SH} &= -Z_{SH}I \\ &= -Z_{SH}(\theta^T\dot{w}+C_p^T\dot{V}_{SH}) \\ &= -Z_{SH}\theta^T sw-Z_{SH}C_{pS}V_{SH} \end{aligned} \tag{16}$$

where s is the Laplace parameter. Therefore, the new defined shunt voltage can be

$$V_{SH}=\frac{-Z_{SH}\theta^T sw}{1+Z_{SH}C_{pS}} \tag{17}$$

Substituting Eq. (17) into the actuator equation [Eq. (14)], the governing equation of a shunted system can be augmented by adding the shunted damping matrix in the Laplace domain :

$$Ms^2w+\left(C+\frac{Z_{SH}\theta\theta^T}{1+Z_{SH}C_{pS}}\right)sw+Kw=f_{ext}(s) \tag{18}$$

The additional damping due to a shunt circuit is added to the inherent damping of a piezo/beam system. In the next section, we will discuss the multimode damping capabilities of the negative capacitive shunting by deriving the transfer function of a cantilevered piezo/beam system.

4. Equations of Motion of a Shunted Piezo/Beam System

A mathematical model is developed to describe

the flexural vibration behavior of a cantilevered piezo/beam system with negative capacitive shunt circuits. The equations of motion of a shunted piezo/beam system are obtained through Hamilton's principle. A schematic configuration of a piezo/beam system with a series and a parallel shunt circuit is shown in Fig. 1. The beam has length l_b, width b_b, thickness h_b, Young's modulus E_b, and mass density ρ_b. The piezoelectric material has thickness h_p, the elastic modulus measured at constant electrical field (e.g., short circuit) E_p^E, and the piezoelectric constants d_{31} in the longitudinal direction.

It is assumed that the transverse displacement, w, of all points on any cross section of piezo/beam layers is considered to be equal. Shear deformation and rotary inertia of the beam and piezo layers are neglected for a Bernoulli-Euler beam. For a symmetric configuration of PZT patches, the net longitudinal displacement of the beam is assumed zero. In addition, the base beam layer and the shunted piezoceramic layers are considered to be perfectly bonded together.

The constitutive equations for a piezoelectric element depends on the mechanical stress, σ, and strain, ε, as well as the electric field, E, and the electric displacement, D. A common form of constitutive equations for passive shunt damping is

$$\begin{bmatrix}\sigma\\ E\end{bmatrix}=\begin{bmatrix}E_s & -h\\ -h & \beta\end{bmatrix}\begin{bmatrix}\varepsilon\\ D\end{bmatrix} \tag{19}$$

where E_s is the elastic modulus at constant displacement, h is the piezoelectric constant, and β is the dielectric constant.

The kinetic energy of a piezo/beam system can be described as

$$T=T_b+2T_p \tag{20}$$

where

$$T_b=\frac{1}{2}\int_0^{l_b}\rho_b A_b\left(\frac{\partial w}{\partial t}\right)^2 dx$$

and

$$T_p=\frac{1}{2}\int_0^{l_b}\rho_p A_p\left(\frac{\partial w}{\partial t}\right)^2[H(x-x_1)-H(x-x_2)]\,dx$$

The strain energy of a piezo/beam system can be described as

$$U=U_b+2U_p \tag{21}$$

where

$$U_b=\frac{1}{2}\int_0^{l_b}E_b I_b\left(\frac{\partial^2 w}{\partial x^2}\right)^2 dx$$

and

$$\begin{aligned}U_p&=\frac{1}{2}\int_V(\varepsilon^T\sigma+ED)\,dV\\&=\frac{1}{2}\int_0^{l_b}\Big[E_p^E I_p\left(\frac{\partial^2 w}{\partial x^2}\right)^2+2A_p h_{31}Dz_n\left(\frac{\partial^2 w}{\partial x^2}\right)\\&\quad+A_p\beta_{33}D^2\Big][H(x-x_1)-H(x-x_2)]\,dx\end{aligned}$$

where $z_n=\frac{1}{2}h_p(h_b+h_p)$ and w is the transverse displacement of the beam. Also, A_b and A_p are the cross sectional area of the beam and the piezo layer, respectively. Furthermore, I_b and I_p are the area moments of inertia about the neutral axis of the each layer. In the above equations, (x_2-x_1) is the length of the PZT patch. The subscripts b and p represent the base beam and the piezoceramic, respectively. The virtual work consists of four terms : the first term is for a work done by the top shunted piezo damper connected to the terminals of a piezoceramic with a resistor-negative capacitor branch circuit in series, the second is due to the bottom shunted piezo damper connected in parallel, the third is due to the external force, and the forth is due to the inherent damping force of a base structure.

$$\delta W=\delta W_{SE}+\delta W_{PA}+\delta W_{ex}+\delta W_{in} \tag{22}$$

where

$$\delta W_{SE}=\left[\left(-R_{SE}+\frac{1}{sC_n}\right)\delta\dot{Q}\right][H(x-x_1)-H(x-x_2)]$$

$$\delta W_{PA}=\left[\left(\frac{-R_{PA}}{1-sC_nR_{PA}}\right)\delta\dot{Q}\right][H(x-x_1)-H(x-x_2)]$$

$$\delta W_{ex}=\int_0^{l_b}f(x,\,t)\,\delta w\,dx$$

$$\delta W_{in}=\int_0^{l_b}c_b\frac{\partial w}{\partial t}\,\delta w\,dx$$

and H is the Heavyside's fuction and Q is the electric charge generated by an external force.

The equations of motion and all the natural and geometric boundary conditions can be obtained by applying the Hamilton's principle

$$\delta H=\delta\int_{t_1}^{t_2}(T-U+W)\,dt=0 \tag{23}$$

where t_1 and t_2 are the end points in the time domain. Substituting the strain energy and kinetic energy into the Hamilton's principle yields the following equation of motion and the electrical circuit equations.

$$\begin{aligned}&\rho_b A_b\left(\frac{\partial^2 w}{\partial t^2}\right)+c_b\left(\frac{\partial w}{\partial t}\right)+E_b I_b\left(\frac{\partial^4 w}{\partial x^4}\right)\\&+2\left[\rho_p A_p\left(\frac{\partial^2 w}{\partial t^2}\right)+E_p^E I_p\left(\frac{\partial^2 w}{\partial x^4}\right)\right][H(x-x_1)-H(x-x_2)]\\&=f(x,t)-\frac{1}{2}b_p h_{31} D_3 h_p(h_b+h_p)\left(\frac{\partial^2}{\partial x^2}[H(x-x_1)-H(x-x_2)]\right)\end{aligned} \tag{24}$$

The electrical circuit equations for a top piezo and a bottom piezo with a resistor-negative capacitor shunt branch circuit are

$$\begin{aligned}&\left[\frac{1}{2}h_{31}h_p(h_b+h_p)\left(\frac{\partial^2 w}{\partial x^2}\right)+\frac{\beta_{33}h_p}{b\ l_p}Q\right.\\&\left.-\left(R_{SE}-\frac{1}{sC_n}\right)\frac{dQ}{dt}\right][H(x-x_1)-H(x-x_2)]=0\end{aligned} \tag{25}$$

$$\begin{aligned}&\left[\frac{1}{2}h_{31}h_p(h_b+h_p)\left(\frac{\partial^2 w}{\partial x^2}\right)+\frac{\beta_{33}h_p}{b\ l_p}Q\right.\\&\left.-\left(\frac{R_{PA}}{1-sC_nR_{PA}}\right)\frac{dQ}{dt}\right][H(x-x_1)-H(x-x_2)]=0\end{aligned} \tag{26}$$

The first terms of Eqs. (25) and (26) define the sensor voltages generated by the curvature of the deformed beam. The second terms are due to the inherent capacitor voltages of piezo patches. The third terms are defined as shunt voltages, which are fed back to piezoceramics.

The assumed modes method is used to discretize the governing equation [Eq. (24)] into a set of ordinary differential equations. The flexural motion for a cantilever beam is approximated by

$$w(x,t)=\sum_{i=1}^{n}\psi_i(x)\,W_i(t)=[\psi]^T[\mathrm{W}] \tag{27}$$

where $\psi_i(x)=\cos\beta_i x-\cos\beta_i x-\sigma_i(\sinh\beta_i x-\sin\beta_i x)$. Here the constants σ_i are the mode shape coefficients (Inman, 1996). Applying mode shape functions to the equation of motion (24) results in the following discretized differential equations of the shunted piezo/beam system:

$$M\ddot{W}(t)+C_b\dot{W}(t)+KW(t)=f_{ext}+f_{piezo} \tag{28}$$

where

$$\begin{aligned}M&=\rho_b A_b\int_0^l\psi_i\psi_i^T dx\\&\quad+2\rho_p A_p\int_0^l\psi_i\psi_i^T[H(x-x_1)-H(x-x_2)]\,dx,\\C_b&=c_b\int_0^l\psi_i'\psi_i'^T x\\K&=E_b I_b\int_0^l\psi_i''\psi_i''^T dx\\&\quad+2E_p^E I_p\int_0^l\psi_i''\psi_i''^T[H(x-x_1)-H(x-x_2)]\,dx\\f_{ext}&=\int_0^l\psi_i f(x,t)\,dx,\\f_{piezo}&=-\frac{1}{2}\left(b_p d_{31}E_p^E V_{SH}^{SE}(h_b+h_p)\int_0^l\psi_i[\delta'(x-x_1)-\delta'(x-x_2)]\right)\\&\quad+b_p d_{31}E_p^E V_{SH}^{PA}(h_b+h_p)\int_0^l\psi_i[\delta'(x-x_1)-\delta'(x-x_2)]\Big)dx\end{aligned}$$

and d_{31} is the piezoelectric material constant. The shunt voltages V_{SH}^{SE} and V_{SH}^{PA} are generated from a series and a parallel resistor-negative capacitor branch circuit.

The charge generated by the PZT patches due to the vibration of the cantilevered piezo/beam can be determined through the integration of the electric field displacement (IEEE, 1978).

$$Q(t)=\int_A DdA \tag{29}$$

with

$$[D]=[d]^T[T]+[\varepsilon]^T[E] \tag{30}$$

$[d]$, $[T]$, $[\varepsilon]$ and $[E]$ represent the piezo-electric strain constant, stress, dielectric permittivity and applied field strength matrix, respectively. Substituting the mode shape function into Eq. (29), the output of a piezo sensor can be derived as follows:

$$\begin{aligned}Q_i(t)=&[2C_0D_n+C_p^T(V_{SH}^{SE}+V_{SH}^{PA})]\\&[H(x-x_1)-H(x-x_2)]\end{aligned} \tag{31}$$

where

$$C_0=d_{31}E_p^E b_p\left(\frac{h_b+h_p}{2}\right)$$

and

$$D_n=\int_0^l\frac{\partial^2\psi_i}{\partial^2 x}[H(x-x_1)-H(x-x_2)]\,dx$$

The current across PZT electrodes can be obtained from the induced charge of the piezoceramic sensor as follows:

$$I_i(t)=\frac{dQ_i}{dt}=[2C_0D_n\dot{W}_n(t)+C_p^T(\dot{V}_{SH}^{SE}+\dot{V}_{SH}^{PA})]\,[H(x-x_1)-(x-x_2)] \quad (32)$$

According to Eq. (5), the shunt voltages are given by:

In the series connection,

$$V_{SH}^{SE}=-Z_{SH}^{SE}I_i(t)=-\left(R_{SE}-\frac{1}{sC_n}\right)\{C_0D_n\dot{W}_n(t)+C_p^TsV_{SH}^{SE}\}\,[H(x-x_1)-H(x-x_2)] \quad (33)$$

In the parallel connection,

$$V_{SH}^{PA}=-Z_{SH}^{PA}I_i(t)=-\left(\frac{R_{PA}}{1-sC_nR_{PA}}\right)\{C_0D_n\dot{W}_n(t)+C_p^TsV_{SH}^{SE}\}\,[H(x-x_1)-H(x-x_2)] \quad (34)$$

The shunt voltages can be rewritten after equating the inherent capacitance of PZTs, C_p, to the external negative capacitance, $-C_n$.

$$V_{SH}^{SE}=-\left(\frac{1-sC_pR_{SE}}{s^2C_p^2R_{SE}}\right)C_0D_n\dot{W}_i(t) \quad (35)$$

$$V_{SH}^{PA}=-R_{PA}C_0D_n\dot{W}_i(t) \quad (36)$$

Substituting these shunt voltages into the piezo force f_{piezo} in Eq. (28), the final form of the governing equations are given by

$$M\ddot{W}(t)+C_{total}\dot{W}(t)+KW(t)=f_{ext} \quad (37)$$

where

$$C_{total}=C_b+f_{piezo}$$

It should be noted here that the piezo shunted force would be an additional damping term of the piezo/beam system and Eq. (37) corresponds to Eq. (18).

5. Theoretical Analyses and Discussions

Theoretical analyses are performed to examine the capabilities of vibration damping control by using two different types of the negative capacitive shunting. A pair of piezoceramics are bonded to each side of the root of the aluminum beam. The edge of the piezoceramic is 0.1 cm away from the fixed end of the beam. The piezoceramic is poled through their thickness and elongate lengthwise so that they are operating in transverse mode ($d_{31}=-320$E-12). The beam is grounded and the two terminals of the top piezoceramic are connected with a series resistor-negative capacitor branch circuit while those of the bottom piezoceramic are connected with it in parallel as shown in Fig. 1. Table 1 lists the physical and geometrical parameters of the aluminum beam and piezoceramic.

A negative capacitive shunting is applied theoretically to reduce the multimode vibration amplitudes of a cantilever beam over a broad frequency range. Figure 5 shows the analytical output response of the shunted piezo/beam system constructed by implementing the series resistor-

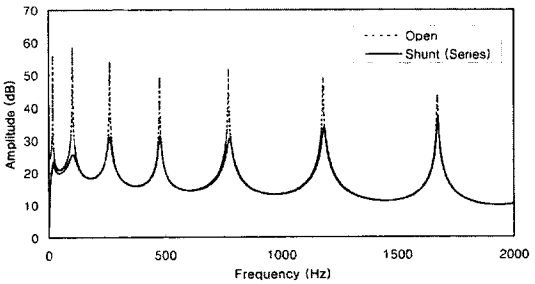

Fig. 5 Analytical frequency response function of shunted piezo/beam system with a series negative capacitive shunting

Table 1 Physical and geometrical properties of the beam and piezoceramic

	Young's Modulus (pa)	Density (Kg/m^3)	Length (m)	Width (m)	Thickness (m)
Aluminum	7.1E10	2700	2.0E-1	2.54E-2	0.8E-3
PZT	6.2E10	7800	4.5E-2	2.54E-2	2.6E-4

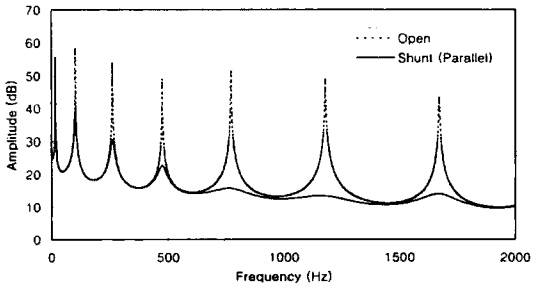

Fig. 6 Analytical frequency response function of shunted piezo/beam system with a parallel negative capacitive shunting

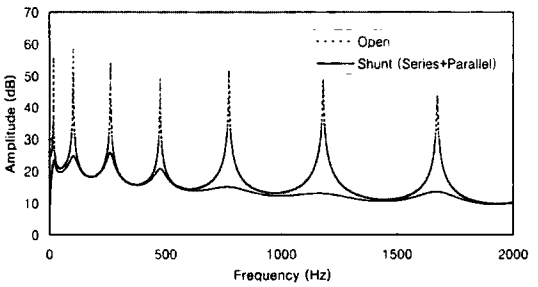

Fig. 7 Analytical frequency response function of shunted piezo/beam system combined a series with a parallel negative capacitive shunting

negative capacitor shunt branch circuit. The vibration amplitude increases as the frequency is increased. This phenomenon is easily explained by considering the material loss factor equation [Eq. (12a)] and Fig. 4(b) for a series resistor-negative capacitor shunt circuit. Ths figure shows that the loss factor of the non-dimensional mechanical impedance decreases as the non-dimensional frequency is increased. In the computer simulation, the resistance of 5 Ohm and the capacitance of 200 nF are used. They are determined by a trial-and-error method.

A parallel resistor-negative capacitive branch circuit is implemented to obtain the behavior of the FRF. Figure 6 shows the analytical transfer response of the shunted piezo/beam system with a parallel resistor-negative capacitor branch circuit. The result shows an opposite behavior in comparison with the series connection case. The vibration amplitude decreases with the increasing frequency. The material loss factor equation [Eq. (12b)] and Fig. 4(b) validate this phenomenon. The loss factor for the parallel resistor-negative capacitor branch circuit increases as the non-dimensional frequency is increased. The resistor value of 200 Ohm and capacitance of 200 nF are used in the simulation. The shunt resistor values used in the series and parallel negative capacitive shunt damper are obtained by a trial-and-error method.

Figure 7 shows the transfer function of the piezo/beam system when a series and a parallel negative capacitive shunting is simultaneously applied. All modes of the system are uniformly suppressed. More specifically, the vibration amplitudes are reduced by more than 25 dB from the pick vibration amplitude of the open circuit across the whole frequency range. It is worthwhile to mention that the effective attenuation of the vibration amplitude is achieved by decreasing the shunt resistance for series shunting and increasing the shunt resistance for parallel shunting. These facts can be explained by considering the relationship between the loss factor and the non-dimensional frequency.

6. Conclusions

A novel multiple-mode vibration damper that combines a series with a parallel negative capacitive shunt circuit has been introduced in this paper. A mathematical model using the assumed mode shape has been developed to describe the flexural vibration of beams subjected to the electromechanical interactions of the piezo/beam system shunted with a series and a parallel resistor-negative capacitive branch circuit. The general modeling of a negative capacitance shunt circuit has been presented by incorporating the feedback shunt voltage generated by the shunt impedance. The top piezoceramic connected with a series resistor-negative capacitor branch circuit is capable of suppressing the vibration amplitudes in the low frequency range. The bottom piezoceramic connected with a parallel resistor-negative capacitor branch circuit is capable of suppressing the vibration amplitudes in the high frequency range. These phenomena can be understood by consi-

dering the stiffness ratio and loss factor with respect to the non-dimensional frequency. By combining the two negative capacitive shunt circuits, a multiple-mode piezoelectric shunted actuator is invented which is capable of suppressing all the structural modes simultaneously. The theoretical results show that the negative capacitive shunting reduces the vibration amplitudes of a piezo/beam system by more than 25 dB over the whole frequency range. Hence, the negative capacitive shunted actuator developed in this study can serve as an invaluable tool for the multimode vibration damping in many engineering applications.

References

Browning, D. R. and Wynn, W. D., 1993, "Multiple-Mode Piezoelectric Passive Damping Experiments for an Elastic Plate," *Proceedings of the 11th International Modal Analysis Conference*, pp. 1520~1526, Kissimmee, FL.

Forward, R. L., 1979, *Electromechanical Transducer-Coupled Mechanical Structure with Negative Capacitance Compensation Circuit*, United States Patent #4158787.

Hagood, N. W., Chung, W. H. and von Flotow, A., 1990, "Modeling of Piezoelectric Actuator Dynamics for Active Structural Control," *Journal of Intelligent Material Systems and Structures*, Vol. 1, pp. 327~354.

Hagood, N. W. and von Flotow, A., 1991, "Damping of Structural Vibrations with Piezoelectric Materials and Passive Electrical Networks," *Journal of Sound and Vibration*, Vol. 146, No. 2, pp. 243~268.

Hollkamp, J. J., 1994, "Multimodal Passive Vibration Suppression with Piezoelectric Materials and Resonant Shunts," *Journal of Intelligent Material Systems and Structures*, Vol. 5, pp. 49~57.

IEEE Std 176-1978, 1978, *IEEE Standard on piezoelectricity*, The Institute of Electrical and Electronics Engineers.

Inman, D. J., 1996, *Engineering Vibration*, Prentice-Hall, Englewood Cliffs NJ.

Lesieutre, G. and Davis, C., 1997, "Can a Coupling Coefficient of a piezoelectric Device be Higher than Those of Its Active Material?," *Proc. of SPIE*, Vol. 3041, pp. 281~292.

Moon, S. H., Yun, C. Y. and Kim, S. J., 2002, "Passive Suppression of Nonlinear Panel Flutter Using Piezoelectric Materials with Resonant Circuit," *KSME International Journal*, Vol. 16, No. 1, pp. 1~12.

Wu, S., 1998, "Method for Multiple Mode Piezoelectric Shunting with Single PZT Transducer for Vibration Control," *Journal of Intelligent Material Systems and Structures*, Vol. 9, pp. 991~998.